

A microfluidic device approach to generate hollow alginate microfibers with controlled wall thickness and inner diameter

Uyen H. T. Pham, Madiha Hanif, Amit Asthana, and Samir M. Iqbal

Citation: [Journal of Applied Physics](#) **117**, 214703 (2015); doi: 10.1063/1.4919361

View online: <http://dx.doi.org/10.1063/1.4919361>

View Table of Contents: <http://scitation.aip.org/content/aip/journal/jap/117/21?ver=pdfcov>

Published by the [AIP Publishing](#)

Articles you may be interested in

[A low cost design and fabrication method for developing a leak proof paper based microfluidic device with customized test zone](#)

Biomicrofluidics **9**, 026502 (2015); 10.1063/1.4918641

[Facile fabrication processes for hydrogel-based microfluidic devices made of natural biopolymers](#)

Biomicrofluidics **8**, 024115 (2014); 10.1063/1.4871936

[A pneumatic valve controlled microdevice for bioanalysis](#)

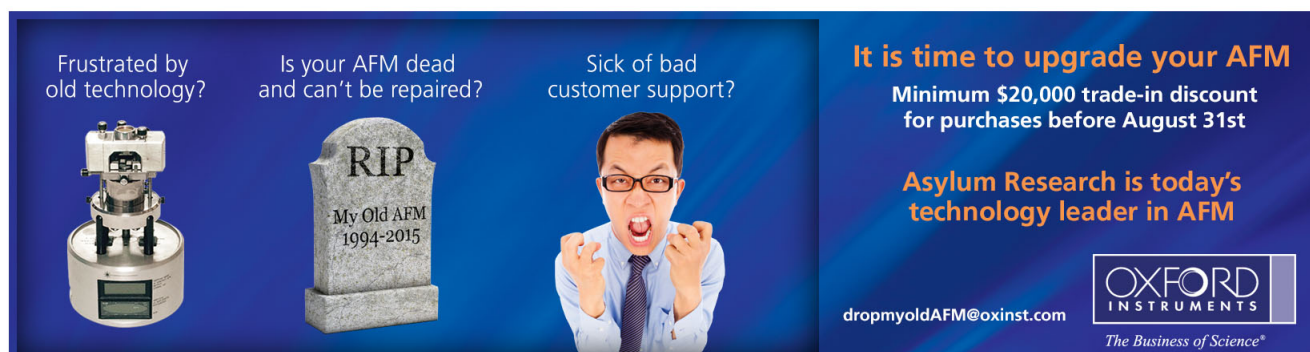
Biomicrofluidics **7**, 054116 (2013); 10.1063/1.4826158

[Bromo-oxidation reaction in enzyme-entrapped alginate hollow microfibers](#)

Biomicrofluidics **5**, 024117 (2011); 10.1063/1.3605512

[Thiolene-based microfluidic flow cells for surface plasmon resonance imaging](#)

Biomicrofluidics **5**, 026501 (2011); 10.1063/1.3596395

The advertisement is set against a dark blue background. On the left, there is a photograph of an old, bulky AFM. In the center, a grey tombstone is shown with the inscription 'RIP My Old AFM 1994-2015'. To the right of the tombstone is a man with glasses, wearing a blue shirt and tie, with a frustrated expression and his hands raised in a 'giving up' gesture. Text on the left side reads: 'Frustrated by old technology?', 'Is your AFM dead and can't be repaired?', and 'Sick of bad customer support?'. On the right side, the text says: 'It is time to upgrade your AFM', 'Minimum \$20,000 trade-in discount for purchases before August 31st', and 'Asylum Research is today's technology leader in AFM'. At the bottom right, the Oxford Instruments logo is displayed with the tagline 'The Business of Science®'. An email address 'dropmyoldAFM@oxinst.com' is also provided.

A microfluidic device approach to generate hollow alginate microfibers with controlled wall thickness and inner diameter

Uyen H. T. Pham,^{1,2,3} Madiha Hanif,^{1,2,3} Amit Asthana,^{4,a)} and Samir M. Iqbal^{1,2,3,5,6,b)}

¹Department of Bioengineering, University of Texas at Arlington, Arlington, Texas 76010, USA

²Nano-Bio Lab, University of Texas at Arlington, Arlington, Texas 76019, USA

³Nanotechnology Research Center, University of Texas at Arlington, Arlington, Texas 76019, USA

⁴CSIR-Centre for Cellular & Molecular Biology, Habsiguda, Uppal Road, Hyderabad – 500 007, India

⁵Department of Electrical Engineering, University of Texas at Arlington, Arlington, Texas 76011, USA

⁶Department of Urology, University of Texas Southwestern Medical Center at Dallas, Dallas, Texas 75235, USA

(Received 26 January 2015; accepted 17 April 2015; published online 3 June 2015)

Alginate is a natural polymer with inherent biocompatibility. A simple polydimethylsiloxane (PDMS) microfluidic device based self-assembled fabrication of alginate hollow microfibers is presented. The inner diameter as well as wall thickness of the microfibers were controlled effortlessly, by altering core and sheath flow rates in the microfluidic channels. The gelation/cross-linking occurred while the solutions were ejected. The microfibers were generated spontaneously, extruding out of the outlet microchannel. It was observed that the outer diameter was independent of the flow rates, while the internal diameter and wall thickness of the hollow fibers were found to be functions of the core and sheath flow rates. At a constant sheath flow, with increasing core flow rates, the internal diameters increased and the wall thicknesses decreased. At a fixed core flow, when sheath flow rate increased, the internal diameters decreased and the wall thickness increased. The immobilization of enzymes in such hollow microfibers can be a potential application as microbioreactors.

© 2015 AIP Publishing LLC. [<http://dx.doi.org/10.1063/1.4919361>]

INTRODUCTION

Alginate is a polysaccharide polymer that is derived from brown algae (Phaeophyceae).¹ Its chemical structure consists of block copolymer of (1,4)- β -D-mannuronate (M) and α -L-guluronate (G) contents.² Alginate hydrogel can be made by different methods such as ionic crosslinking, covalent crosslinking, or thermal gelation. The simplest alginate hydrogel formation is through ionic crosslinking. During gelation, only G blocks crosslink with divalent cations which is described as an “egg-box” model.² Different chemical agents have variety of effects on the gelation of alginate, with calcium chloride (CaCl₂) being the most commonly used. Calcium chloride is a highly water soluble chemical reagent; its Ca²⁺ cations crosslink with alginate via ionic diffusion.³ Moreover, it rapidly increases the gelation rate of the alginate hydrogel. The physical and chemical properties of alginate depend on the source of alginate which may contain various lengths of M and G residue components and selective binding sites for multivalent cations. In addition, the sol-to-gel transition of alginate during gel formation is not affected by temperature. These unique characteristics have made alginate a promising candidate to mimic biological matrices.¹ Alginate hydrogel possesses many natural characteristics that make it the most suitable material for many biological applications such as enzyme immobilization, drug delivery, tissue engineering, food industry, pharmaceutical industry, wound dressing, etc.

Over last two decades, the applications of microstructures like microfibers, microspheres, microstrips, microbeads, etc., have steadily increased in areas like tissue engineering, biotechnology, and analytical chemistry.⁴ The efficiency of chemical functionalization, biocompatible surface derivation, and molecular immobilization depends on the type of microstructures. For example, many studies have demonstrated the encapsulation and culture of cells in the alginate hydrogel microfibers. The common characteristic of the fabricated fiber microstructures for cell culturing is to possess very thin side walls. These fiber-shaped microstructures can be used to mimic the 3D constructs of complex tissues *in vivo* like blood vessels, muscle fiber, neural nerves, etc.⁵ The thin side wall allows the cultured cells to proliferate and migrate into 3D functional morphology. However, these structures are not suitable for enzyme immobilization applications. The thin side walls of the fiber microstructure cause massive and rapid leakage from the microfibers.

Enzyme immobilization is a method to confine enzymes in the supporting matrix. The common microstructures for enzyme immobilization are microbeads or microfibers. It is very difficult to control the gelation rate of microbeads and thus their size distribution lacks uniformity.⁶ The previous studies have reported limitations due to low encapsulation efficiency and diffusion of enzymes through the thin walls of microbeads/microspheres. Therefore, there is a need for a coating of cationic polymer like chitosan.^{7–9} However, the coating layers cause toxicity to the immobilized molecules.¹⁰

Compared to microbeads, microfibers have a larger surface-to-volume ratio. The fiber-based techniques like electrospinning, wet spinning, interfacial complexation, or

^{a)}Email: aa@cmb.res.in.

^{b)}Present address: University of Texas at Arlington, 500 S. Cooper St #217, Box 19072, Arlington, Texas 76019, USA. Email: SMIBAL@uta.edu. Telephone: +1-817-272-0228. Fax: +1-817-272-7458.

thermal spinning have been employed to fabricate the microfibers. The microfibers have been used as substrates or for reinforcement in biotechnology. These production methods are, however, expensive, hard to control, and incompatible with biological molecules due to high electric fields involved or harshness of the chemical agents used.¹¹

In this work, the micro-devices were fabricated and used for facile synthesis of hollow alginate microfibers. As compared to other fiber-based techniques, the microfluidic platform is: (1) simple, (2) rapid, and (3) provided superior control over microfiber properties. In the present method no chemical agents or high electric fields were employed to generate microfibers. The microfibers were fabricated in the microfluidic channels by coaxial flow reaction. Divalent cations exchange and crosslink with pre-polymer chains to form the microfiber structure. The fibers were generated spontaneously and extruded out of the channel after certain residence time. Traditionally, soft lithography is used to fabricate complex devices. For example, Kang¹² designed a single microfluidic device that contained coaxial-flow channels and rectangular channels. While rectangular channels could be fabricated easily, cylindrical channels require templates that can be removed after polymer gelation. In addition, the process of fabricating rectangular and cylindrical microchannels by soft lithography is time consuming and not suitable for a wet lab environment due to the requirement of cleanroom and specialized tools.

In 2004, Jeong *et al.*¹³ introduced a new method to fabricate the cylindrical microchannels using embedded glass capillaries. The glass capillary-based platform has been used to fabricate poly (lactic-co-glycolic acid) (PLGA) microfibers for 3D cell culture,¹⁴ alginate microfibers for cellular loading,⁴ and to create microfibers to control the cell orientation.¹⁵ With the glass capillary-based systems, the fabricated microfibers contained thin side walls. Thus these fibers could only be used for cell harvesting. Moreover, changing the flow rate controlled the outer diameter of the generated microfibers. The glass capillary-based system is simple and rapid, however, it is labor-intensive, requires certain skill sets and the use of specialized tools.¹² Moreover, none of the previous studies have reported the relationship between flow rates and internal diameter or wall thickness of hollow microfibers.

In this paper, we introduce a PDMS microfluidic device fabricated using an embedded template method.^{8,16} Unlike the glass capillary-based platform, our microfluidic devices were fabricated completely in PDMS. The bench-top embedded template method of fabrication was simple, rapid, and cost-effective. This device was then used to generate long continuous hollow microfibers. The inner diameters and the wall thickness of alginate hollow microfibers were controlled by changing the flow rates. The alginate microfibers were characterized for their diameters and the wall thicknesses with respect to the core and sheath flow rate. We show that: (1) at a constant sheath flow with an increasing core flow, the internal diameters increased and wall thicknesses decreased; and (2) at a constant core flow with an increasing sheath flow, the internal diameters decreased and the wall thicknesses increased.

EXPERIMENTAL

Materials

PDMS was prepared using Sylgard 184 kits purchased from Ellsworth Adhesives (Dow Corning, Midland, MI, USA). The kit contained PDMS base and curing agent. Sodium alginate (Protanal LF 10/60 FT, high gel-strength and medium viscosity, pH 6.0–8.0 of 1% solution) was a gift from FMC BioPolymer (Philadelphia, PA, USA). Anhydrous calcium chloride (BioReagent, $\geq 96.0\%$) was obtained from Sigma-Aldrich (St. Louis, MO, USA).

Fabrication of PDMS microfluidic device

The design of the microfluidic device was a “diverged Y-shape.” This was an optimum design because it qualified the following criteria: (1) all pre-polymer and chemical agents merged at the intersection, and (2) it prevented back-flow through the inlets. The microfluidic device was fabricated by a simple embedded template method described by Asthana *et al.*¹⁶ The device contained three inlets and one outlet port (Fig. 1). The three inlets were connected 1 mm away from the end of the outlet microchannel.

As indicated in Fig. 2, the outlet template was a plastic hollow capillary tube with an outer diameter of 0.7 mm. A small hole was punched through the plastic hollow capillary using a small BD needle (26 G \times 5/8 in.). The distance from one end of the plastic tube to the punched hole was 1 mm. A long straight aluminium wire was introduced through the hole. The diameter of the wire was 0.4 mm.

This wire was bent at approximately 45° to form a V-shape. For the main inlet template, another wire was attached at the end of the plastic hollow tube. Larger 1 mm diameter plastic hollow capillaries were placed at the open-end of three inlets and outlet.

As shown in Fig. 2, the embedded template was secured on the Petri dish using double-side tape. The mixture of PDMS pre-polymer and curing agent (ratio 10:1) was poured to completely cover the template. The whole assembly was put in a vacuum chamber for degassing. The Petri dish with the template covered in PDMS was then cured at 150 °C. Thereafter, all the templates were pulled out from the cured PDMS matrix followed by oxygen plasma exposure of as-fabricated device for 10–15 min. The oxygen plasma treatment made the PDMS surface hydrophilic due to the introduction of silanol (Si—OH) groups to the surface.

Synthesis of hollow alginate microfibers

For fabrication of the alginate hollow fibers, the experiment was set up as shown in Fig. 3. The alginate microfiber was generated in a microfluidic device using coaxial-flow inflow ionic crosslinking. A 2% alginate solution (w/v) was run through the side channels as sheath flow. A 20 mM CaCl₂ aqueous solution was introduced from the central channel as core flow. When the three fluids merged at the intersection, the gelation mechanism spontaneously began and ionic crosslinking occurred between sodium alginate and calcium chloride. The unreacted CaCl₂ diffused through to the walls of the hollow fiber walls and acted as a lubricant, which

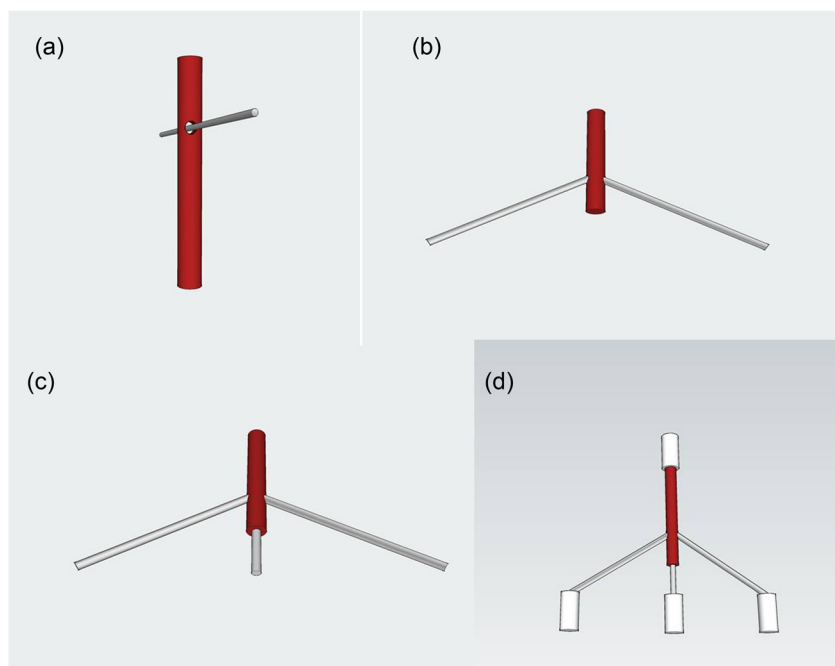


FIG. 1. The template method. (a) The aluminium wire was inserted through the hole. (b) The wire was bent to form a V-shape. (c) The single wire was attached at other end of the plastic tube. (d) The large plastic tubes were placed at the open end of inlets and outlet.

assisted in smooth extrusion of hollow fibers from the outlet channel without requiring any additional pressure.⁴ By adjusting the flow rates of CaCl_2 core and alginate sheath

flow easily controlled the diameter of the alginate hollow microfiber. The relationships between the flow rates and diameters of the hollow microfibers were investigated by two sets of experiments: (1) changing core flow at a fixed sheath flow rate, and (2) changing the sheath flow at a constant core flow rate.

In the first set of experiments, the sheath flow was kept constant at 0.05 ml/min while the core flow was changed to 0.42, 0.50, 0.75, and 0.90 ml/min. In the second set of

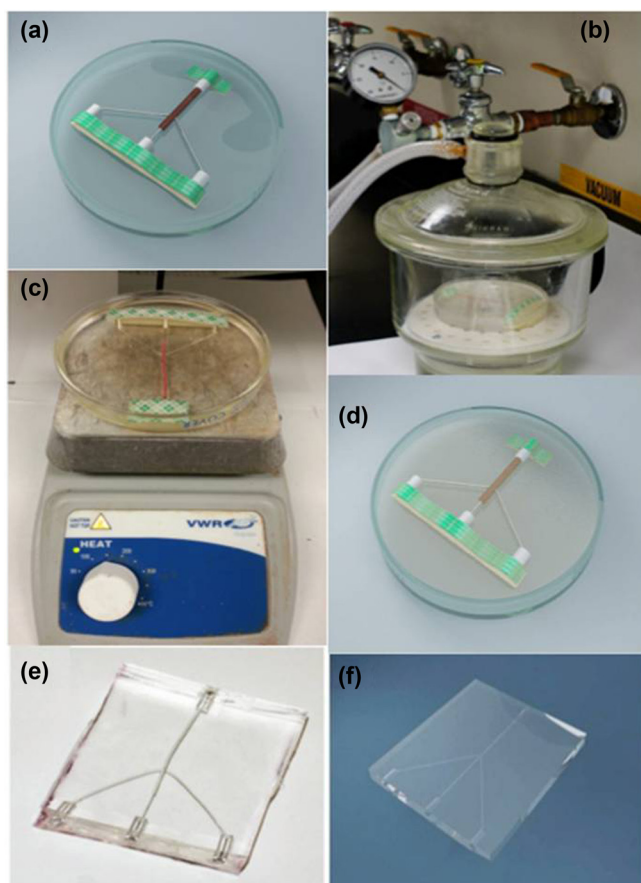


FIG. 2. Bench-top fabrication of the microfluidic device. (a) The diverged Y-shape template platform has three inlet ports and one outlet. (b) The template is fully covered by PDMS prepolymer and then placed in a vacuum chamber. (c) The assembly is cured at 150°C. (d)–(f) The templates are pulled out leaving voids which work as microfluidic channels.

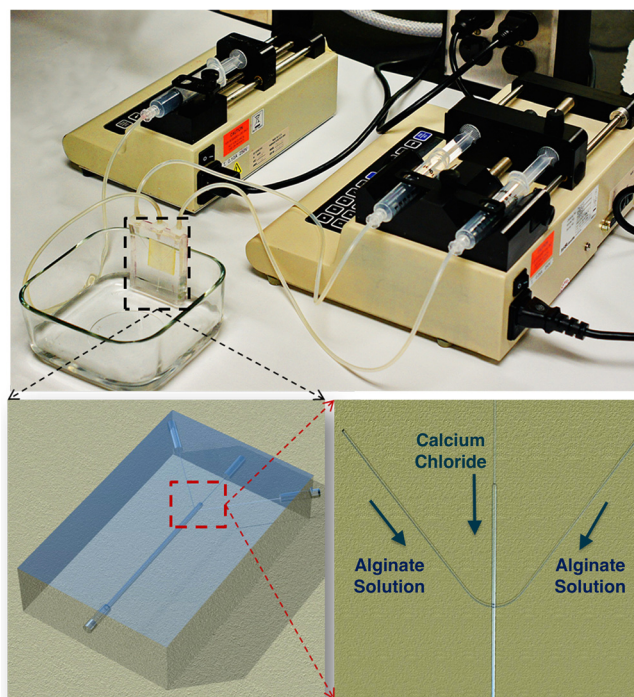


FIG. 3. The experiment setup. A 2% alginate solution is introduced from the two side-channels and 20 mM CaCl_2 is injected from the central channel. The alginate and CaCl_2 solutions merge at the intersection and crosslink. The hollow microfiber is collected in a beaker of 100 mM CaCl_2 solution.

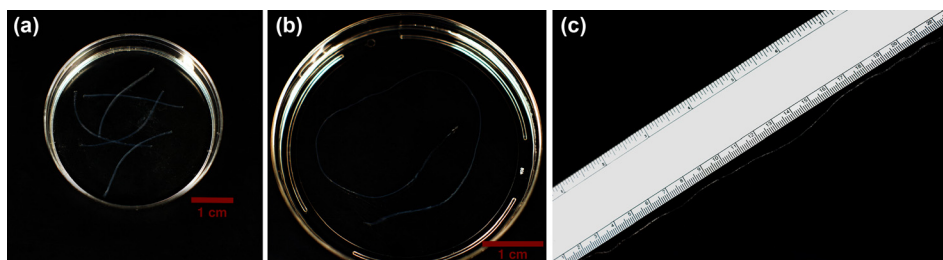


FIG. 4. The length of the generated microfiber is easy to control: (a) 4–6 cm. (b) and (c) A 22 cm long microfiber.

experiments, the sheath flow was changed to 0.01, 0.03, 0.05, 0.1, and 0.3 ml/min while the core flow was fixed at 0.50 ml/min. The fabricated alginate fibers were immersed in a 100 mM CaCl_2 solution for 24 h to harden the microfibers.

For diameter and wall thickness characterization, the fibers were imaged using an optical microscope. The lengths of the fibers were kept at 4–6 cm, while the internal and outer diameters were measured randomly at 10 different points on the fiber. The wall thickness was calculated by subtracting the internal diameter from the outer diameter. Each flow rate experiment was repeated at least three times. The fiber diameter characterizations were expressed as the mean and standard deviation. Linear relationships were seen between the flow rates and the microfiber diameters.

RESULTS AND DISCUSSION

Characterization of hollow alginate microfiber

The single long hollow microfiber could be fabricated continuously as long as the solutions were fed at the inlet ports. As an example, microfibers of 4 and 22 cm length are shown in Fig. 4. If required, longer hollow microfibers can also be generated.

The hollow and symmetric characteristics of the generated microfiber are indicated in Fig. 5 micrographs. The internal diameters and the wall thicknesses are clearly distinguishable. In Fig. 5(c), the outer wall of the hollow

microfiber is stained and this clearly delineates the core of the fiber. As observed in Fig. 5(d), the core space of the microfiber is smooth and it shows no signs of rupture or clogging.

Varying core flow rates at constant sheath flow rate

It was observed that the variation in the core flow rates, while keeping sheath flow constant, had definite effect on the inner diameter and wall thickness of the alginate hollow microfibers (Fig. 6). The relationship between flow rates and inner diameter of the fibers was observed to be linear. At a constant sheath flow, when the core flow rate increased, the internal diameter also increased while the wall thickness decreased.

However, outer diameter was found to be independent of the core flow rate and negligible change in outer diameter was observed. The change in internal diameter and wall thickness with increasing core flow rates is shown in Fig. 6. The internal diameter was smallest at 0.42 ml/min and largest at 0.90 ml/min.

Until date, there exists little information on the decrease in the wall thickness with an increasing core flow rate. The most reasonable explanation is based on the velocity profile

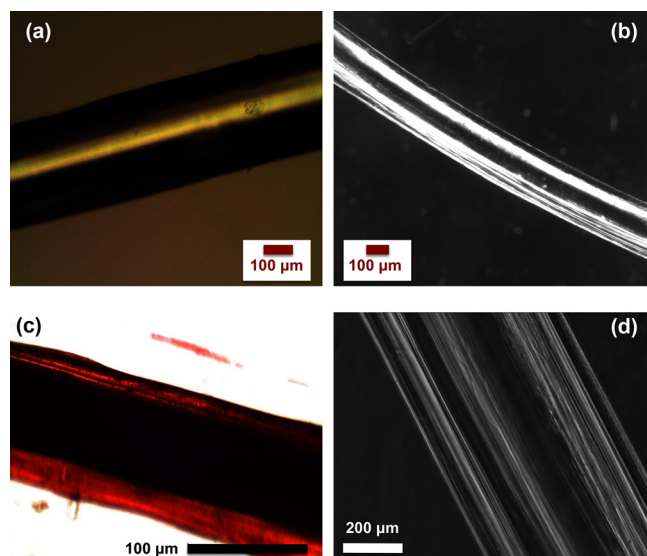


FIG. 5. The core diameter of the hollow microfiber is distinguishable from the outer diameter as shown by (a) and (b) optical micrographs. (c) The fluorescent micrograph of a dried alginate fiber. (d) There is no clogging inside the microfiber.

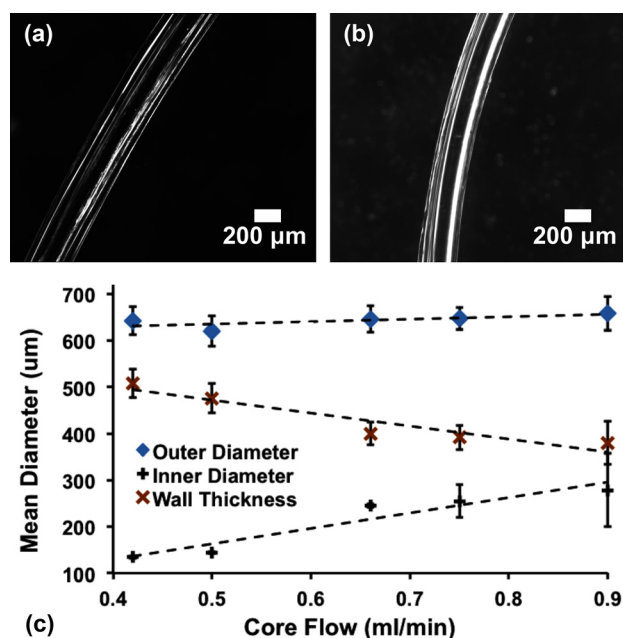


FIG. 6. (a) At 0.42 ml/min, the internal diameter is $134 \pm 2.75 \mu\text{m}$. (b) At 0.90 ml/min, the internal diameter is approximately $278 \pm 78.83 \mu\text{m}$, while keeping the sheath flow constant at 0.05 ml/min. (c) The graph shows the dependence of internal diameter and wall thickness of hollow fibers on core flow at a constant sheath flow of 0.05 ml/min ($n = 3$).

concept.^{17,18} At a constant sheath flow rate, with increasing core flow rates, the velocity profiles between the core and sheath flows are significantly different. This difference causes increase in drag force of the two fluids that results in the stretching of the core fluid. This phenomenon causes decrease in diffusion of Ca^{2+} , which leads to less effective crosslinking between Ca^{2+} and alginate, resulting in a thin fiber wall at a high core flow rate. Another possible explanation of thinner wall of hollow fiber is shift in the focus of sheath flow. At core flow rates lower than the constant sheath flow, sheath flow has focusing or pinching effect similar to hydrodynamic focusing in droplet generation. On the other hand, at higher core flow rates, this focusing reduces and core flow pushes the sheath flow towards the wall of the microfluidic device causing thinner walls. To further explore the above explanation series of experiments were done with varying sheath flows at constant core flow, as described below.

Effect of changing sheath flow at constant core flow rate

Here again, a linear relationship between flow rates and inner diameter as well with wall thickness of the hollow microfibers was observed (Fig. 7). The outer diameter of the hollow fiber was clearly independent of the sheath flow rate, while the internal diameter decreased and wall thickness increased with increasing sheath flow rates. Once again, based on the velocity profile and hydrodynamic focusing, the relationship of sheath flow and the dimension of the fiber can be explained. In the case of increasing sheath flow at a

constant core flow rate, the core flow was more focused. This resulted in an increase of surface contact between the two fluids. The Ca^{2+} divalent cations thus rapidly cross-linked with the carboxylic group of sodium alginate via diffusion. Therefore, it generated a thicker side wall with a decrease in the inner diameter. It was observed that internal diameter reached a minimum of $95 \pm 24.1 \mu\text{m}$ at 0.3 ml/min and a maximum of $252 \pm 26.2 \mu\text{m}$ at 0.01 ml/min of sheath flow rate while keeping the core flow rate constant (Fig. 7).

Earlier reports have indicated that the size of the fabricated microfiber can be controlled only by retooling the needles or embedded glass pipettes.¹⁷ On the other hand, another study has reported that the wall thickness of the fabricated fiber cannot be controlled by flow rate.¹⁸ But here we have demonstrated that the flow rates can be effectively used to control the dimensions of the microfibers including the wall thickness without any specialized tools or retooling of needles.

In many recent studies, the microfiber is generated by using a glass capillary/pipettes based system.^{4,7,13–15} Compared to the traditional soft lithography or photolithography techniques, the glass capillary-based microfluidic device is simpler and more rapid. However, this technique requires specialized equipment, such as microforge and microcapillary puller. While in this work, a very simple method of embedded template is demonstrated to fabricate PDMS microfluidic device without any requirement of specialized equipment and facilities. The fabrication process can be done in a simple bench-top manner. In the case of the

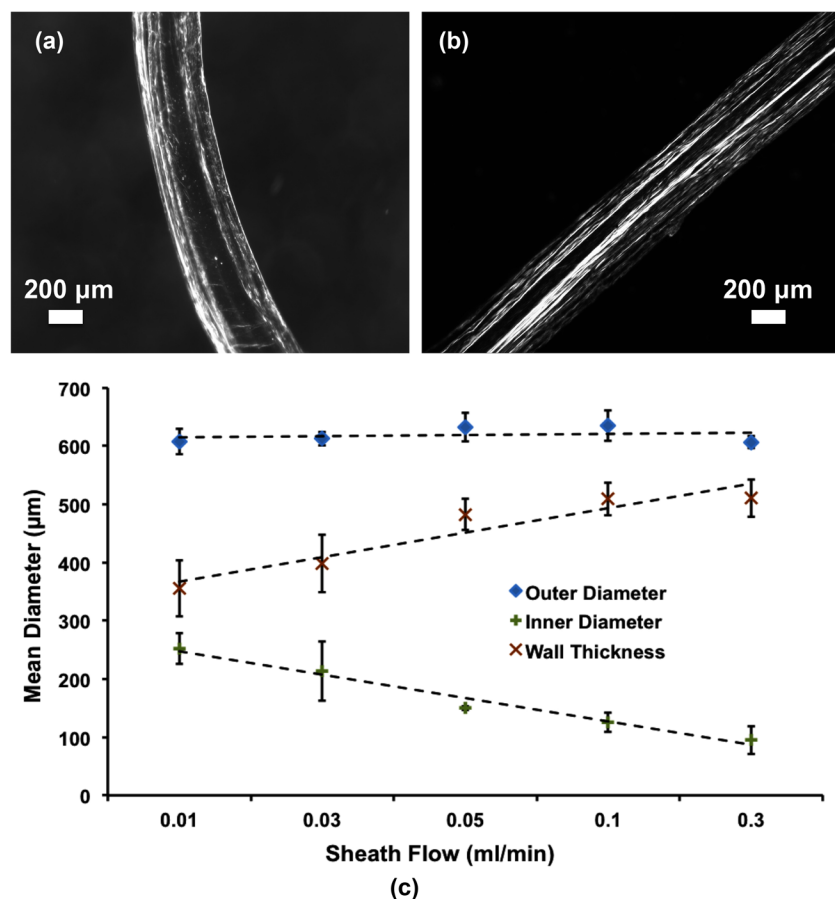


FIG. 7. The internal diameter is (a) largest at 0.01 ml/min and (b) smallest at 0.3 ml/min . (c) at a constant core flow rate of 0.5 ml/min , the inner diameter and wall thickness changes with the sheath flow rate ($n = 3$).

glass capillary-based systems, the controllable flow rates must be kept in narrow optimal ranges to avoid a spiral curl of the fiber. The formation of spiral curl by the microfiber can lead to clogging of the microchannel outlet. For example, as reported by Shin *et al.*,⁴ in order to fabricate a straight microfiber, the optimal CaCl_2 sheath flow and alginate sample flow were 20 ml/min and 1 $\mu\text{l}/\text{min}$. Compared to previous works, our technique is more efficient and easier to use. The ranges of the flow rates are more flexible and the spiral curl does not occur even at extremely high flow rates. For instance, in our experiment, the highest alginate and CaCl_2 flow rates were 0.3 ml/min and 0.9 ml/min. The advantage of this wide range of flow rates is that it will be a rapid process when fabricating microfibers on a large scale with varying dimensions irrespective of applications.

CONCLUSIONS

This work demonstrates a simple embedded template method to fabricate PDMS microfluidic device without the need for cleanroom or specialized equipment. The microfluidic devices used for the synthesis of alginate microfibers are very simple and provide rapid means to generate microfibers. The size of the fiber (diameters and wall thickness) is controlled by merely changing the flow rates. The advantage of this technique is that it can be used extensively for fabrication of bioreactors, and can be used for continuous monitoring of analytes, their concentration, biotransformations, and chemical synthesis.

ACKNOWLEDGMENTS

The authors acknowledge experimental assistance and useful discussion with Young-Tae Kim, Mohammad R. Hasan, Jeyantt S. Sankaran, Muhymun Islam, Wintana T. Kansai, Phuong M. Nguyen, Dien V. Nguyen, and Thong Trinh. This work was supported by the National Science Foundation through an REU Supplement to grant ECCS-1201878.

¹K. I. Draget and C. Taylor, "Chemical, physical and biological properties of alginates and their biomedical implications," *Food Hydrocolloids* **25**(2), 251–256 (2011).

²K. Y. Lee and D. J. Mooney, "Alginate: properties and biomedical applications," *Prog. Polym. Sci.* **37**(1), 106–126 (2012).

³K. I. Draget, "Alginates," in *Handbook of Hydrocolloids*, 2nd ed., edited by G. O. Phillips and P. A. Williams (Woodhead Publishing, 2009), pp. 807–828.

⁴S.-J. Shin, J.-Y. Park, J.-Y. Lee, H. Park, Y.-D. Park, K.-B. Lee, C.-M. Whang, and S.-H. Lee, "'On the fly' continuous generation of alginate fibers using a microfluidic device," *Langmuir* **23**(17), 9104–9108 (2007).

⁵H. Onoe, T. Okitsu, A. Itou, M. Kato-Negishi, R. Gojo, D. Kiriya, K. Sato, S. Miura, S. Iwanaga, and K. Kuribayashi-Shigetomi, "Metre-long cell-laden microfibres exhibit tissue morphologies and functions," *Nat. Mater.* **12**(6), 584–590 (2013).

⁶A. Ilyas, M. Islam, W. Asghar, J. U. Menon, A. S. Wadajkar, K. T. Nguyen, and S. M. Iqbal, "Salt-leaching synthesis of porous PLGA nanoparticles," *IEEE Trans. Nanotechnol.* **12**(6), 1082–1088 (2013).

⁷A. Asthana, K. H. Lee, K.-O. Kim, J. Perumal, L. Butler, S.-H. Lee, and D.-P. Kim, "Bromo-oxidation reaction in enzyme-entrapped alginate hollow microfibers," *Biomicrofluidics* **5**, 024117 (2011).

⁸A. Asthana, K. H. Lee, K.-O. Kim, D.-M. Kim, and D.-P. Kim, "Rapid and cost-effective fabrication of selectively permeable calcium-alginate microfluidic device using 'modified' embedded template method," *Biomicrofluidics* **6**, 012821 (2012).

⁹Q. Liu, A. M. Rauth, and X. Y. Wu, "Immobilization and bioactivity of glucose oxidase in hydrogel microspheres formulated by an emulsification-internal gelation-adsorption-polyelectrolyte coating method," *Int. J. Pharm.* **339**(1), 148–156 (2007).

¹⁰Y. A. Morch, I. Donati, B. L. Strand, and G. Skjåk-Bræk, "Effect of Ca^{2+} , Ba^{2+} , and Sr^{2+} on alginate microbeads," *Biomacromolecules* **7**(5), 1471–1480 (2006).

¹¹A. Tamayol, M. Akbari, N. Annabi, A. Paul, A. Khademhosseini, and D. Juncker, "Fiber-based tissue engineering: Progress, challenges, and opportunities," *Biotechnol. Adv.* **31**(5), 669–687 (2013).

¹²E. Kang, "Novel PDMS cylindrical channels that generate coaxial flow, and application to fabrication of microfibers and particles," *Lab Chip* **10**(14), 1856–1861 (2010).

¹³W. Jeong, J. Kim, S. Kim, S. Lee, G. Mensing, and D. J. Beebe, "Hydrodynamic microfabrication via 'on the fly' photopolymerization of microscale fibers and tubes," *Lab Chip* **4**(6), 576–580 (2004).

¹⁴C. M. Hwang, A. Khademhosseini, Y. Park, K. Sun, and S.-H. Lee, "Microfluidic chip-based fabrication of PLGA microfiber scaffolds for tissue engineering," *Langmuir* **24**(13), 6845–6851 (2008).

¹⁵C. M. Hwang, Y. Park, J. Y. Park, K. Lee, K. Sun, A. Khademhosseini, and S. H. Lee, "Controlled cellular orientation on PLGA microfibers with defined diameters," *Biomed. Microdevices* **11**(4), 739–746 (2009).

¹⁶A. Asthana, K.-O. Kim, J. Perumal, D.-M. Kim, and D.-P. Kim, "Facile single step fabrication of microchannels with varying size," *Lab Chip* **9**(8), 1138–1142 (2009).

¹⁷T. Takei, S. Sakai, H. Ijima, and K. Kawakami, "Development of mammalian cell-enclosing calcium-alginate hydrogel fibers in a co-flowing stream," *Biotechnol. J.* **1**(9), 1014–1017 (2006).

¹⁸S. Sakai, Y. Liu, E. J. Mah, and M. Taya, "Horseradish peroxidase/catalase-mediated cell-laden alginate-based hydrogel tube production in two-phase coaxial flow of aqueous solutions for filament-like tissues fabrication," *Biofabrication* **5**(1), 015012 (2013).